AN ABSOLUTE METHOD FOR AEROSOL PARTICLE MASS MEASUREMENT

by

MARK ANDREW PHILIP

B.Sc(Eng)., University of the Witwatersrand
(1979)

SUBMITTED TO THE DEPARTMENT OF CHEMICAL ENGINEERING IN PARTIAL FULFILLMENT OF THE REQUIREMENTS FOR THE DEGREE OF:

MASTER OF SCIENCE IN CHEMICAL ENGINEERING

at the

MASSACHUSETTS INSTITUTE OF TECHNOLOGY

October 1981

Signature of Author _____
Department of Chemical Engineering
October 28, 1981

Certified by _____
Fred Gelbard
Thesis Supervisor

Accepted by _____
Glenn C. Williams
Chairman, Department Committee

TABLE OF CONTENTS

AN ABSOLUTE METHOD FOR AEROSOL PARTICLE MASS MEASUREMENT

by

MARK A. PHILIP

Submitted to the Department of Chemical Engineering
on October 28, 1981, in partial fulfillment of the
requirements for the Degree of Master of Science in
Chemical Engineering
at the Massachusetts Institute of Technology

ABSTRACT

An absolute method for aerosol particle mass measurement has been developed. The method involves suspension of a charged particle in an electrodynamic chamber called a quadrapole. From the voltage required to balance the particle against gravity, the particle charge-to-mass ratio can be measured. By irradiating the particle with UV light, a single electron can be removed and a new balancing voltage determined. From the balancing voltage measured before and after this so-called process of "electron stepping", the particle mass and charge are determined absolutely without knowledge of the particle shape, density or any adjustable parameters. Application of the method on calibration particles of 2.35 ± 0.0197 μm in diameter gave measured particle diameters of 2.339 ± 0.014 μm, which was well within the manufacturer's stated standard deviation. Excellent reproducibility was obtained for different particles of the same size.

Thesis Supervisor: Prof. Fred Gelbard
Title: DuPont Assistant Professor
of Chemical Engineering

ACKNOWLEDGEMENTS

Few students can have been as fortunate as I have been to work with a supervisor of the caliber of Prof. Fred Gelbard. His unfailing support and enthusiasm helped carry this work through a number of frustrating periods. His accessibility and his insight made this thesis a rewarding and educational experience.

I am also most fortunate to have known a number of good friends and helpful colleagues, whose support and encouragement I value greatly. Among these, I thank Pablo Debenedetti, Ted Nunn, Martiel Luther, Patrick van de Weijer, Vince Paul, Horacio Valeiras and Howard Bernstein.

I thank Prof. Steven Arnold of the Polytechnic Institute of New York for his advice on the practical aspects of electrodynamic chambers and for his loan of an electrodynamic chamber. I thank John McCarthy of the Materials Science Department of M.I.T. for his advice on aerosol generation. I thank Larry Johnson for the typing of this manuscript.

This research was supported by the National Institute of Health and the M.I.T. Energy Laboratory.

I am indebted to my father, whose foresight and persistence persuaded me to take up this venture and to him and my mother I owe heartfelt thanks for their support and encouragement during my time at M.I.T.

LIST OF FIGURES

LIST OF TABLES

LIST OF SYMBOLS

a dimensionless parameter in modified Mathieu Equation

$\bar{a}$ dimensionless parameter in Mathieu Equation

a_{2n} constants in solution to Mathieu Equation

A_n constants in solution to endcap dc field

b_{2n} constants in solution to Mathieu Equation

B_n constants in solution to endcap dc field

C geometric constant of endcap dc field

C_d drag coefficient

C_s slip correction factor

C_{2r} constants in solution to Mathieu Equation

d particle diameter

$D(t)$ displacement of particle from geometric center of chamber

D_o constant in solution to Mathieu Equation - displacement of center of motion of particle

E electric field

$f(t)$ solution to Mathieu Equation

$f(\tau)$ solution to Mathieu Equation

F dimensionless force

g acceleration due to gravity

k dimensionless drag parameter

m particle mass

n number of charges on particle

P_n Legendre Polynomial of n^{th} order

q particle charge

r radial direction

r_s radial direction, spherical co-ordinates

R dimensionless radial distance

t time

V potential difference

z axial direction

z_o characteristic dimension of electrodynamic chamber

Z dimensionless axial distance

Greek

β parameter in solution to Mathieu Equation

δ multiplicative constant

ε elementary unit of charge

γ fractional error

η viscosity

Ω frequency

μ parameter in solution to Mathieu Equation

τ dimensionless time

Subscripts

ac alternating current

dc direct current

f final

g gravitational; used to denote endcap potential difference and electric field

i initial

1. INTRODUCTION

Air pollutants may be classified as gaseous or aerosol. Both pollutant forms may be directly emitted into the atmosphere or formed there from the reactions of gaseous precursors. Homogeneous gas phase reactions may yield a variety of gaseous pollutants, but often the products are condensible species which subsequently form an aerosol. Existing aerosols, whether emitted directly from a source or formed from gaseous precursors, may undergo heterogeneous gas/aerosol particle reactions. Such reactions generally result in growth of the aerosol particle and are usually referred to as gas-to-particle conversion processes. Although much work has been reported on elucidating the mechanisms of gas-to-particle conversion, the heterogeneous mechanisms are not completely understood. Clearly, an understanding of gas-to-particle conversion processes is necessary for the development of atmospheric pollution models and environmental control strategies.

Particle growth by gas-to-particle conversion results from the diffusion of gaseous molecules to the particle, with subsequent incorporation of these molecules into the particle by condensation and/or chemical reaction (35,36). Several theoretical growth rate calculations have been reported (4,16,20,36,37), but accurate growth rate measurements are needed to provide kinetic data and to verify or invalidate existing models. For experimental determination of particle growth rates, one would like the experimental conditions to correspond as closely as possible to those found in the atmosphere. In particular the

desired experimental technique should

1) contain the particles without the use of supporting structures which may contaminate or interfere with the particle;
2) suspend single particles, thereby eliminating the complex sampling and analytical procedures required for multi-particle systems and the accounting for aerosol interactions with the containment chamber walls;
3) suspend the particle in a controlled environment for residence times of several hours;
4) perform direct mass measurements on a particle with a temporal resolution of less than about a minute;
5) be capable of determining the mass of non-spherical particles such as those found in the atmosphere;
6) be capable of measuring variations in mass of sub-micron particles as found in the atmosphere;
7) not be restricted to mass measurements requiring *a priori* knowledge of the particle (e.g. composition, diameter or density).

Previous approaches to measuring particle growth rates will now be reviewed in light of the above seven criteria and a summary of the ensuing discussion is given in Table 1.1.

One of the most simple and direct methods of measuring gas-to-particle conversion rates is to use bulk quantities of material and measure bulk changes in mass as a function of time as the material is exposed to a known gas composition. Such an approach has been used by Cofer et al.(2,23). In their experiments, changes in mass are measured on carbon black dusted over a small weighing pan of a microbalance and exposed to a

Portions of the text on the
following page(s) are not legible
in the original.

TABLE 1.1 Previous Work on the Measurement of Gas-to-Particle Conversion Rates

*see text

TECHNIQUE	(1) No supporting structure*	(2) Single Particle	(3) Long residence time	(4) Short temporal resolution	(5) Non-spherical particles	(6) Submicron particles	(7)* No a priori knowledge	SYSTEMS STUDIED	INVESTIGATORS
Bulk micro-balance weighing			✓	✓	✓		✓	Carbon black dusted on a weighing pan and exposed to reacting atmosphere. Measurement of change of particle mass.	2,23
Deposited bulk material			✓		✓			Solid deposited on filter paper exposed to reacting environment. Measurement of change in gas composition.	10,11
					✓			Tubular flow reactor with interior surface coated with bulk solid. Measurement of change in gas composition.	8
Packed bed				✓	✓			Fixed bed reactor with Teflon beads onto which were deposited discrete aerosol particles. Measurement of change in gas composition. System may suffer from additional mass transfer resistance due to the packed bed.	9
Aerosol Chamber									
Batch	✓		✓	✓	✓	✓		Soot aerosol generated by burner and fed to reaction chamber. Aerosol particles submicron. Measurement of change in gas composition with time from periodic sampling of chamber.	6
Flow	✓				✓	✓		Submicron aerosol fed continuously to reactor along with reacting atmosphere. Measurement of change in gas composition.	16
Single droplet	✓	✓						Large (700-900 μm) single droplets exposed to reacting atmosphere. Measurement of change of gas composition. Extrapolation of results to submicron particles necessary.	5
Electro-dynamic containment chamber									
Science Spectrum Differential II	✓	✓	✓	✓		✓		Flat plate chamber with pin electrode to levitate and center single particles into laser beam for light scattering measurement of particle diameter. Feedback system necessary to keep particle in laser path.	40
Quadrapole	✓	✓	✓	✓		✓		Chamber uses hyperboloidal electrodes to focus particle at center of chamber. Initial diameter obtained by light scattering. Particle charge-to-mass ratio obtained by applying dc potential across endcap electrodes. Particle mass obtained by comparison of charge-to-mass ratio at any time with initial charge-to-mass ratio and initial mass computed from initial diameter.	14,30
Flat plate with electron stepping	✓	✓	✓	✓	✓	✓	✓	Flat plate chamber levitates particle. Particle charge-to-mass ratio obtained from balancing potential. Single electron removed from particle with UV light. Knowledge of initial and final charge-to-mass ratios allows calculation of particle mass. Feedback system necessary.	15

reacting atmosphere. Although these experiments may provide much information, the experimental conditions may not adequately simulate the highly dispersed conditions of atmospheric aerosols. The same comments may be made about the work of Judeikis et al. (8), who use a tubular flow reactor with a layer of solids deposited on the inner cylindrical surface. Chun et al.(10) and Dyson et al.(11), who deposit thin layers of Fe_2O_3 or ZnO on filter paper, have similar limitations in their approach. Corn and Cheng (9) use a system consisting of a fixed bed reactor packed with Teflon beads onto which have been deposited discrete aerosol particles. Two limitations of this system are the additional mass transfer resistance of the packed bed and that particles' surface properties may have been altered by their deposition on the beads. Some experimenters have employed reacting aerosol systems. Britton et al.(6) use soot generated by a burner and carried into a reaction chamber for exposure to a reacting environment. The system operates in batch mode, but offers a limited residence time. Data is obtained by periodic sampling. Because of the nature of the soot this system also suffers from difficulties in characterizing the aerosol soot. Matteson et al.(16) use a system employing a continuous flow of aerosol through a reaction chamber. This severely limits their reaction time to about 15 minutes. Because of the large number of simultaneously reacting particles and the continuous aerosol flow, changes in gas composition must be measured, giving indirect measurement of rates of change of mass. However, both Britton and Matteson study submicron particles in the

size range found in the atmosphere. Johnstone et al.(5) study single droplets, exposing these to controlled reacting environments and measuring rates of absorption of gas. However, the droplets used were very large, 700 to 900 μm in diameter, which required extrapolation to atmospheric conditions.

Techniques using single particles of the order of 1 μm in diameter have been reported by Wyatt and Phillips(40), Davis and Ray (14,30) and Arnold (15). These investigators employ electrodynamic containment chambers, which utilize the residual charge found on aerosols, to contain single particles. Wyatt and Phillips have reported on a commercial instrument, the Science Spectrum Differential II. This instrument employs two flat circular plates and a small pin electrode. Application of a dc voltage across the plates levitates the charged particle and application of a dc voltage to the pin centers the particle into a laser beam. A servomechanism is required to maintain the particle within the laser beam. Particle diameter is obtained by light scattering measurements,and given the density, particle mass can be computed. This technique has two distinct advantages: It observes small particles freely suspended in a gas and is thus capable of well replicating particles in the atmosphere. Further, it allows study of reactions over a period of days. However, the light scattering technique is relatively tedious compared to another technique (electron stepping),does not provide direct measurement of mass, and is not suitable for non-spherical particles. Also, the particle within the device is on a potential hill in that once disturbed from its equilibrium, it continues to move away from equilibrium. Thus

a feedback system and servomechanism are necessary to keep the particle constantly balanced in the laser beam. Davis and Ray use a different electrodynamic chamber, hereinafter referred to as the "quadrapole". The quadrapole consists of two hyperboloidal endcap electrodes and a central ring electrode having a hyperboloidal cross section. An exploded view of the quadrapole is presented in Fig.1.1 and a cross section in Fig. 2.1. Application of an ac voltage to the ring electrode produces an electric field having a time-averaged focussing effect towards a well defined null point at the geometric center of the chamber. Thus a charged particle within the field, is subject to a net (time-averaged) force towards the null point. Because of gravity, a charged particle will be held somewhat below the geometric center of the chamber. By applying a dc potential across the endcap electrodes one can return the particle back to the geometric center of the chamber and thus directly measure the charge-to-mass ratio of the particle from this balancing dc potential. Weurker et al.(27) report that this concept was first used by Paul and Raether (25) in their "electric mass filter" and that a similar system was used by Fischer (26) to contain electrons and ions. Weurker et al.report developing the quadrapole to the extent that they are able to suspend small, charged metallic particles of the order of several microns in diameter in a vacuum. They also add a dc bias to the ac voltage on the ring electrode in an effort to improve particle containment. Blau et al. (28)have built a quadrapole in which they study light scattering by particles ranging from 7.5 μm to 110 μm in diameter. Good agreement between experiment and

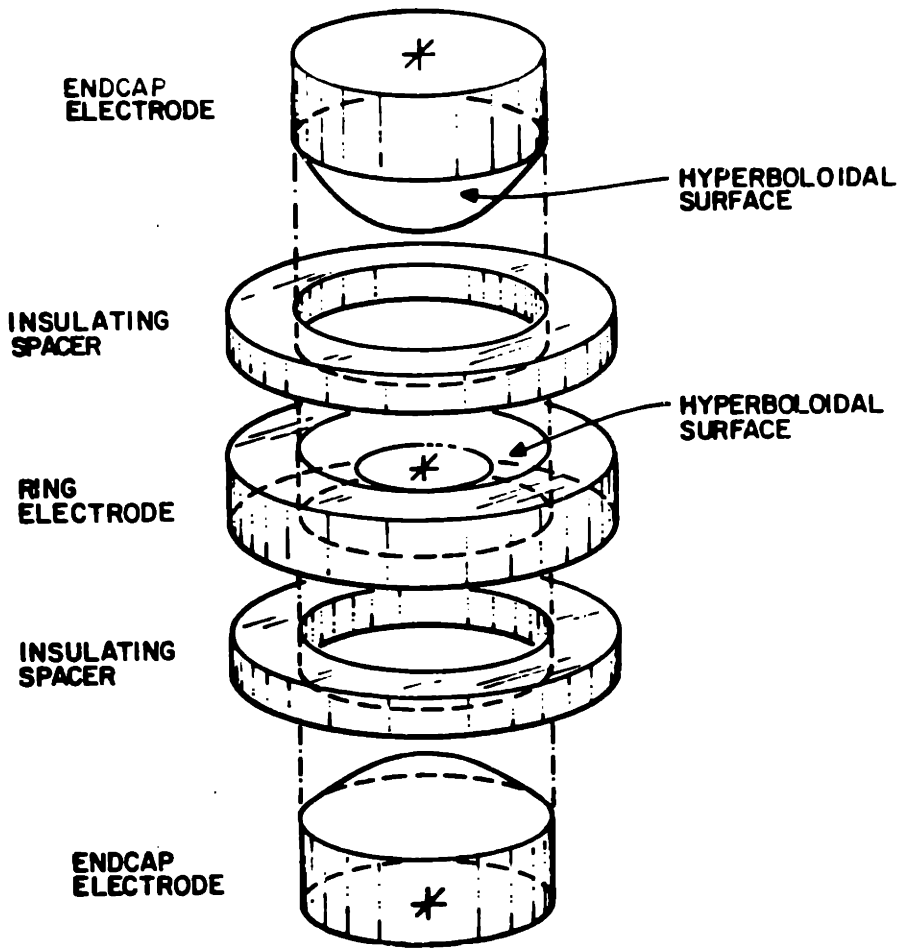

FIG. I.I EXPLODED VIEW OF QUADROPOLE

Mie theory is reported. Frickel et al. (29) study aerosol containment using bihemispherical and bihyperboloidal electrodes. They present a comprehensive solution to and discussion of the governing equations of motion and report experimental verification of predicted particle behaviour. Ray (14,30) also presents a shorter solution to the governing equations. The quadrapole allows study of single aerosol particles freely suspended in a gas and it has the advantage that a particle within the chamber is in a time-averaged potential well. Thus once disturbed from equilibrium at the null point, the particle experiences restorative forces which increase in magnitude the further the particle moves from the null point. Therefore, within limits, the quadrapole will tend to contain particles even when they are not balanced at the null point and will return a disturbed particle back to its point of balance at the null point. Feedback systems are not necessary. Davis and Ray use light scattering to determine the initial diameter of their particle. The initial mass is computed using an assumed density and the initial balancing dc voltage across the endcaps is noted. They then note the balancing voltage V_g as a function of time and obtain the particle mass as a function of time by comparing V_g at any time with the initial value of V_g. They do not check the particle diameter for consistency with the mass data. This method implicitly assumes that the number of charges on the particle remains constant and that the particle density remains constant during the experiment. As regards particle density, a particle undergoing reaction may change its density with time. Estimates of loss of charge by negatively charged par-

ticles through cosmic ray ionization, range from one elementary unit per day for small particles several microns in diameter (31) to about 3 elementary units of charge per second over a period of 3 days for a highly charged 66.7 μm polyethylene bead (29). As with Wyatt's technique, light scattering is relatively tedious, does not provide direct measurement of mass and is not suited to handling non-spherical particles. Arnold (15) utilizes a simpler flat plate geometry, called a "Milliken Balance", to balance a particle against gravity by means of a dc voltage applied across the plates. The particle charge-to-mass ratio is directly obtained as the plate separation-to-applied voltage ratio multiplied by the acceleration due to gravity. The particle is then irradiated with UV light to remove a single electron, after which the particle is rebalanced to obtain a new charge-to-mass ratio. Assuming the charge on the particle differs by one elementary unit, the particle mass is easily obtained from the two charge-to-mass ratios. This technique is hereinafter referred to as "electron stepping". This system is very simple and the direct measurement of mass eliminates the need for the detailed information about particle shape required for sedimentation or light scattering measurements. Arnold's system is thus not limited to spherical particles. However, as with Wyatt's system, a feedback system is needed to keep the particle constantly balanced.

The purpose of this thesis is to investigate the feasibility of using electron stepping in a quadrapole to measure the mass of a single particle as a function of time. This experimental system has all the seven desirable features

given above for measuring gas-to-particle conversion rates. In addition, no feedback mechanism is required to contain a particle.

In Chapter 2 of this thesis a detailed discussion of the theory of the quadrapole is given. From the analysis, the regions of stable particle behavior and the design criteria are obtained. Further, it is shown that electron stepping in the quadrapole may be used to obtain an accurate measurement of particle mass. In Chapter 3, experimental methods are described and discussed. In Chapter 4, measurements are presented of the mass of diagnostic particles for the purpose of testing and evaluating the technique. In Chapter 5, the significance of these data is discussed and recommendations for future developments of the system are given.

2. THEORETICAL DISCUSSION OF THE ELECTRODYNAMIC BALANCE

2.1 Governing Equations

As shown in Figure 2.1, the chamber is cylindrically symmetric. The inner surfaces of the endcap electrodes are given by

$$z^2 = \frac{r^2}{2} + z_0^2 \tag{2.1}$$

where z is the vertical distance from the geometric center of the chamber and r is the radial distance from the axis of symmetry. The characteristic dimension of the chamber is z_0, half the distance between the two endcap electrodes, measured along the axis of symmetry. The inner surface of the ring electrode is given by

$$z^2 = \frac{r^2}{2} - z_0^2 \tag{2.2}$$

Assuming that potentials V_0 and $-V_0$ are applied to the ring and endcap electrodes respectively, the potential field within the chamber is governed by Laplace's Equation

$$\frac{1}{r}\frac{\partial}{\partial r}\left(r\frac{\partial V}{\partial r}\right) + \frac{\partial^2 V}{\partial z^2} = 0 \tag{2.3}$$

subject to

$$V = V_0 \text{ at } z^2 = \frac{r^2}{2} - z_0^2 \tag{2.4}$$

$$V = -V_0 \text{ at } z^2 = \frac{r^2}{2} + z_0^2 \tag{2.5}$$

By direct substitution into Equations (2.3),(2.4) and (2.5), it can be shown that

$$V(z,r) = -\frac{V_0}{z_0^2}\left(z^2 - \frac{r^2}{2}\right) \tag{2.6}$$

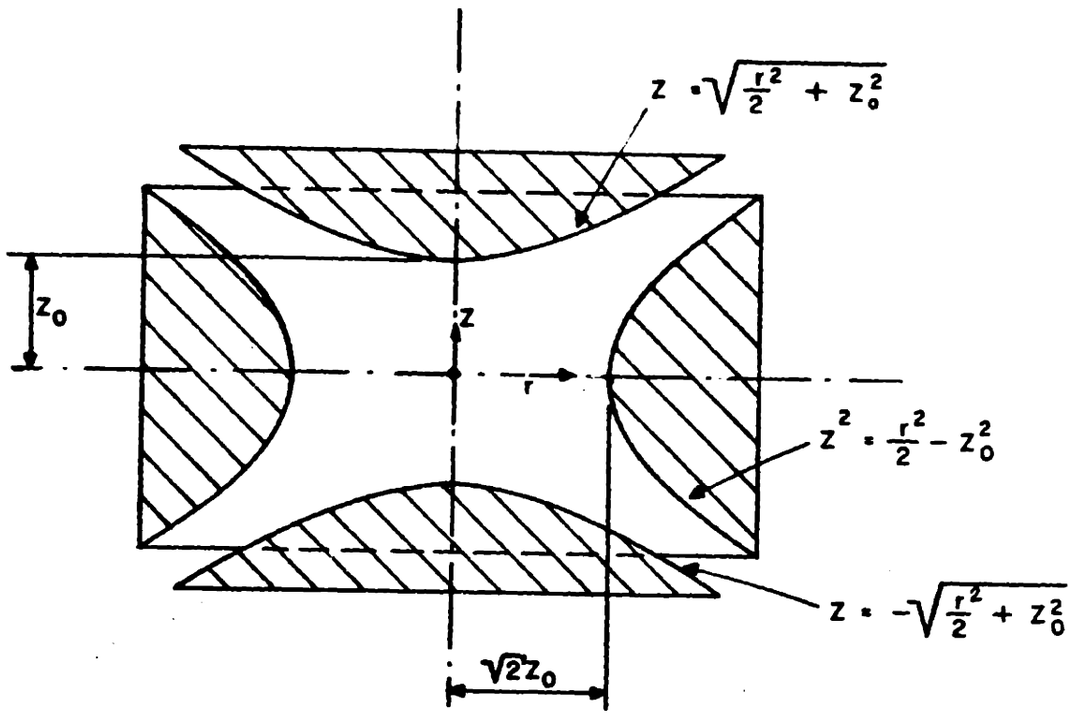

FIG 2.1 CROSS SECTION OF QUADRAPOLE

For a time varying potential $V_0(t)$, applied to the ring electrode, the potential field is given by Eq. (2.6) with $V_0(t)$ substituted for V_0. Since the electric field is equal to minus the gradient of the potential, the electric fields in the radial and axial direction respectively are given by

$$E_r = - \frac{V_0(t) r}{z_0^2} \tag{2.7}$$

$$E_z = \frac{2V_0(t) z}{z_0^2} \tag{2.8}$$

Note that due to cylindrical symmetry, there is no electric field in the angular direction. In this work, the voltage applied to the ring electrode is given by

$$V_0(t) = V_{dc} + V_{ac} \cos(\Omega t) \tag{2.9}$$

where V_{dc}, V_{ac} and Ω are constants. Superimposed on the field formed due to the potential given by Eq. (2.9) is an electric field produced by applying a dc voltage V_g across the endcap electrodes. At the origin (i.e. r = 0 and z = 0), this field, by symmetry, is only in the z direction and is given by

$$E_g = \frac{CV_g}{z_0} \tag{2.10}$$

where C is a geometrical constant, equal to 0.5 for two infinite flat plates. As shown in Appendix A, Eq. (2.10) is a good approximation for small values of z/z_0 and r/z_0.

Consider a particle with charge q and mass m within the chamber. Momentum balances in the z and r direction give

$$m \frac{d^2z}{dt^2} + C_d \frac{dz}{dt} - qE_z + mg - qE_g = 0 \tag{2.11}$$

$$m \frac{d^2 r}{dt^2} + C_d \frac{dr}{dt} - qE_r = 0 \qquad (2.12)$$

Where C_d is the drag coefficient, equal to $3\pi\eta d/C_s$ for a particle of diameter d in a medium with viscosity η and undergoing Stoke's flow. The slip correction factor C_s is given by Friedlander (35). By defining the following dimensionless variables

$$\tau = \frac{\Omega t}{2} \qquad (2.13)$$

$$Z = \frac{z}{z_0} \qquad (2.14)$$

$$R = \frac{r}{z_0} \qquad \text{and} \qquad (2.15)$$

substituting Eq. (2.9) into Eqs. (2.7) and (2.8), Eqs. (2.11) and (2.12) can be written as

$$\frac{d^2 Z}{d\tau^2} + 2\left[\frac{C_d}{m\Omega}\right]\frac{dZ}{d\tau} - 2\left[\frac{4qV_{dc}}{m\Omega^2 z_0^2}\right]Z \qquad (2.16)$$

$$- \frac{8qV_{ac}}{m\Omega^2 z_0^2}\cos(2\tau)Z + \frac{4}{\Omega^2 z_0^2}\left[gz_0 - \frac{qCV_g}{m}\right] = 0$$

$$\frac{d^2 R}{d\tau^2} + \frac{2C_d}{m\Omega}\frac{dR}{d\tau} + \frac{4qV_{dc}R}{\Omega^2 m z_0^2} + \frac{4qV_{ac}\cos(2\tau)R}{\Omega^2 m z_0^2} = 0 \qquad (2.17)$$

By defining the following dimensionless groups

$$k = \frac{C_d}{m\Omega} \qquad (2.18)$$

$$\bar{q}_z = -2\bar{q}_r = \frac{4qV_{ac}}{\Omega^2 m z_0^2} \qquad (2.19)$$

$$\bar{a}_z = -2\bar{a}_r = -\frac{8qV_{dc}}{\Omega^2 m z_0^2} \qquad (2.20)$$

$$F = -\frac{4}{\Omega^2 z_0^2}\left[gz_0 - \frac{qCV_g}{m}\right] \qquad (2.21)$$

Equations (2.16) and (2.17) reduce to

$$\frac{d^2Z}{d\tau^2} + 2k\frac{dZ}{d\tau} + [\bar{a}_z - 2\bar{q}_z\cos(2\tau)]Z = F \tag{2.22}$$

$$\frac{d^2R}{d\tau^2} + 2k\frac{dR}{d\tau} + [\bar{a}_r - 2\bar{q}_r\cos(2\tau)]R = 0 \tag{2.23}$$

Note that Eq. (2.22) is independent of R and Eq. (2.23) is independent of Z. Thus the particle motions in the z and r directions are mutually independent. If we let

$$Z = e^{-k\tau}[f_1(\tau)+f_p(\tau)] \tag{2.24}$$

and

$$R = e^{-k\tau}f_2(\tau) \tag{2.25}$$

Eqs. (2.22) and (2.23) reduce to the inhomogeneous and homogeneous forms of the Mathieu Equation, respectively.

$$\frac{d^2f_p}{d\tau^2} + [a-2\bar{q}\cos(2\tau)]f_p = Fe^{k\tau} \tag{2.26}$$

$$\frac{d^2f_2}{d\tau^2} + [a-2\bar{q}\cos(2\tau)]f_2 = 0 \tag{2.27}$$

where $a = \bar{a} - k^2$.

The solution to this equation is discussed in detail by McLachlan (32) and also by Frickel (29). A different approach to the solution to this equation is presented by Zaroodny (33). Using the general solution to Eq. (2.27) as given by McLachlan (32) and Frickel (29), we have that

$$R = e^{-k\tau}\left[A_1e^{\mu\tau}\sum_{r=-\infty}^{\infty}C_{2r}e^{2r\tau i} + B_1e^{-\mu\tau}\sum_{r=-\infty}^{\infty}C_{2r}e^{-2r\tau i}\right]$$

$$Z = e^{-k\tau}\left[A_2e^{\mu\tau}\sum_{r=-\infty}^{\infty}C_{2r}e^{2r\tau i} + B_2e^{-\mu\tau}\sum_{r=-\infty}^{\infty}C_{2r}e^{-2r\tau i}\right] \tag{2.28}$$

$$+ D_0 + \sum_{n=1}^{\infty} (a_{2n}^2+b_{2n}^2)^{1/2} \cos[2n\tau-\tan^{-1}(\frac{b_{2n}}{a_{2n}})] \qquad (2.29)$$

where C_{2r}, a_{2n}, b_{2n}, D_o, A,B are constants and μ is a parameter, the value of which depends on the values of a and $\bar{q}$. The values of the C_{2r} depend on the values of a and $\bar{q}$, while the a_{2n} and b_{2n} and D_o depend on a, $\bar{q}$, and F. A,B are determined only by initial conditions.

We are interested in stable containment of the particle and hence in stable solutions to Eq. (2.27). McLachlan discusses the stability of the Mathieu Equation and demonstrates that the stability of Eq. (2.27) depends on a and $\bar{q}$. From McLachlan, we have that if a and $\bar{q}$ lie in a stable region, then Eq. (2.28) reduces to the stable solution

$$R = A_1 e^{-k\tau} \sum_{r=-\infty}^{\infty} C_{2r} \cos(2r+\beta)\tau + B_1 e^{-k\tau} \sum_{r=-\infty}^{\infty} C_{2r} \sin(2r+\beta)\tau \qquad (2.30)$$

where β is a parameter, the value of which depends on a and $\bar{q}$. If a and $\bar{q}$ lie in an unstable region, then from Eq. (2.28), we note that if $k>\mu>0$ and k is positive, R is stable, whereas if $0\leq k<\mu$, R is unstable. Thus R is stable if a and $\bar{q}$ lie in a stable region of the $a-\bar{q}$ plane or, if a, $\bar{q}$ lie in an unstable region but $k>\mu$. From Eq. (2.29), we note that the particular integral

$$D_0 + \sum_{n=1}^{\infty} (a_{2n}^2 + b_{2n}^2)^{1/2} \cos(2n\tau-\tan^{-1} \frac{b_{2n}}{a_{2n}}) \qquad (2.31)$$

is always stable. Thus Z is stable under the same conditions as for R. McLachlan (in Chapter 4) presents stable and unstable regions of the $a-\bar{q}$ plane and also methods for calculating the parameter μ.

For convenience, let us first consider the case in which

$V_{dc} = 0$ such that $\bar{a}_r = \bar{a}_z = 0$. The consequences of setting $V_{dc} = 0$ will be discussed later (Frickel presents the analysis for non-zero V_{dc}). With this simplification, $a = -k^2$. Using McLachlan's stability diagram and his calculation of the parameter μ, the regions of stable behaviour of R and Z on the $k-\bar{q}$ plane are shown in Fig. 2.2. Fig. 2.2. agrees closely with similar plots presented by Frickel and Davis and Ray (14,30). Clearly if R or Z is unstable, a particle will not be contained by the chamber. However, if both R and Z are stable, then permanent containment of the particle is possible. Under stable conditions, we see from Eq. (2.29) that as τ increases, R tends to zero and Z tends to just the particular integral Eq. (2.31). Thus the steady-state behaviour of a contained particle is given by

$$R = 0 \tag{2.32}$$

$$Z = D_0 + \sum_{n=1}^{\infty} (a_{2n}^2 + b_{2n}^2)^{1/2} \cos(2n\tau - \tan^{-1}\frac{b_{2n}}{a_{2n}}) \tag{2.33}$$

The series in Eq. (2.33) may be approximated by taking only the first term. Frickel (29) presents a convenient method for evaluating D_o and the constants a_{2n} and b_{2n}. Using Frickel's approach and taking only the first term of the series, we have that the dimensionless vertical displacement is given by

$$Z \approx \frac{2F}{\bar{q}_z^2}(1+k^2) + \frac{F}{\bar{q}_z}(1+k^2)^{1/2}\cos(2\tau - \tan^{-1}k) \tag{2.34}$$

Since gravity does not displace the particle horizontally from the chamber center, only the vertical displacement is considered. In terms of measured quantities, the vertical displacement from the chamber center is given by

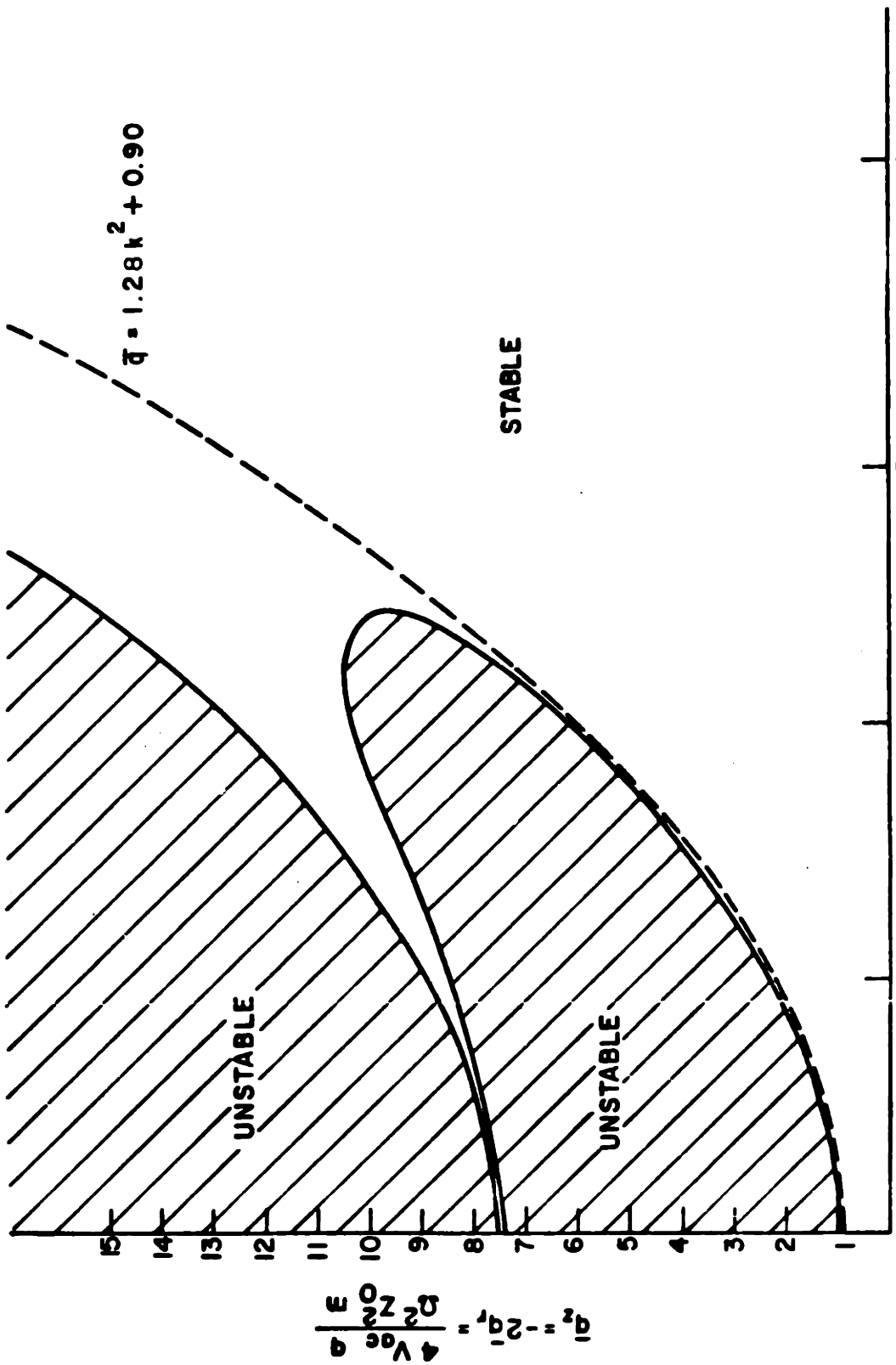

FIG 2.2 STABILITY DIAGRAM FOR THE SOLUTION TO MATHIEU EQUATION (Eq. 2-27)

$$D \approx -\frac{z_0^3}{2(q/m)V_{ac}^2}\left[\frac{gz_0}{(q/m)} - CV_g\right]\left[\Omega^2+\left(\frac{C_d}{m}\right)^2\right]$$

$$-\frac{z_o}{V_{ac}\Omega}\left[\frac{gz_0}{(q/m)} - CV_g\right]\left(\Omega^2+\left(\frac{C_d}{m}\right)^2\right)^{1/2}\cos\left(\Omega t-\tan^{-1}\frac{C_d}{m\Omega}\right) \qquad (2.35)$$

From Eq. (2.35) we see that the particle oscillates vertically with the center of motion above or below the null point if CV_g is greater or less than $gz_0/(q/m)$, respectively. If the particle is balanced, $CV_g = gz_0/(q/m)$, and the center of motion coincides with the center of the chamber. For a balanced particle the amplitude of oscillation is zero and thus the particle is stationary at the center of the chamber. We note that there is a phase lag between the oscillation of the particle and the driving ac voltage.

We now consider the effect on the particle of non-zero values of V_{dc}. Consider a negatively charged particle near the ring electrode which has a positive dc voltage placed on it. The ring electrode can be viewed essentially as a ring of charge. Thus a negative particle displaced above or below the ring will experience an attractive force toward the plane of the ring (34). The electric field due to the ring decreases with increasing distance from the plane of the ring. Thus there is a limited distance from the ring within which the particle will experience a significant attractive force toward the ring. The effect of V_{dc} on the ring electrode is thus to improve the focussing effect in the z direction of the ac voltage. Therefore by neglecting V_{dc} in the equations (which will be used later for design purposes), we are calculating a conservative estimate of the ability of the chamber to contain particles. Thus retaining V_{dc}

(i.e. setting $\bar{a} \neq o$) does not alter the form of the solutions given in Eq. (2.35), but does alter the evaluation of the coefficients D_o, a_{2n}, b_{2n}. In summary, by neglecting V_{dc} in the design equations, conservative estimates for stability are obtained.

2.2 Electron Stepping

A particle with n+1 charges is balanced with a balancing voltage V_g, given by

$$V_g = \frac{g z_o m}{C\varepsilon(n+1)} \tag{2.36}$$

where ε is the elementary charge, equal to 1.602×10^{-19} coulombs. If the particle is irradiated with ultraviolet light such that only n charges remain on the particle, the resulting displacement from the center is given by Eq. (2.35) with V_g given by Eq. (2.36). Thus the displacement after removal of an electron is given by

$$D = -\frac{z_0^4 m^2 g}{2\varepsilon^2 V_{ac}^2 n^2(n+1)} \left[\Omega^2 + \left(\frac{C_d}{m}\right)^2\right] \tag{2.37}$$
$$- \frac{z_0^2 g m}{V_{ac} \Omega \varepsilon n(n+1)} \left[\Omega^2 + \left(\frac{C_d}{m}\right)^2\right]^{1/2} \cos\left[\Omega t - \tan^{-1}\left(\frac{C_d}{m\Omega}\right)\right]$$

Thus once an electron has been removed from an initially balanced (and therefore stationary) particle, it is displaced from the chamber center and it oscillates, as given by Eq. (2.37).

2.3 Design Criteria

2.3.1 Stable Containment of Particles

From the stability diagram given in Fig. 2.2, we see that for $\bar{q} < 15$, a conservative approximation of the stability boundary

may be given by

$$\bar{q} = 1.28\ k^2 + 0.90 \tag{2.38}$$

such that the particle is stable for

$$\bar{q} < 1.28\ k^2 + 0.90 \tag{2.39}$$

For $\bar{q} = \bar{q}_z$, using Eqs. (2.18) and (2.19) we have that, for ε positive

$$nV_{ac} < \frac{0.320C_d^2 z_0^2}{m\varepsilon} + \frac{0.225\Omega^2 m z_0^2}{\varepsilon} \tag{2.40}$$

and for $\bar{q} = -2\bar{q}_r$

$$nV_{ac} > -\frac{0.640C_d^2 z_0^2}{m\varepsilon} - \frac{0.450\Omega^2 m z_0^2}{\varepsilon} \tag{2.41}$$

where n is the number of charges on the particle and ε is the elementary electric charge of $\pm$ 1.602 x 10^{-19} coulombs. Note that since n, V_{ac}, z_o, m and ε are all positive quantities, Eq. (2.41) is always satisfied and thus Eq. (2.40) establishes a design criterion. For ε negative, we find a less restrictive design criterion and so Eq. (2.40) establishes the most restrictive design criterion.

2.3.2 Initial Containment of Particles

When the particle is first introduced it will be contained if the sum of the displacement of the center of motion and the amplitude of oscillation is less than z_o. Using Eq. (2.35), we set the sum of the displacement of center of motion and the amplitude of oscillation to be less than z_o. This leads to a quadratic in V_{ac}. Solving this quadratic and noting that V_{ac} is positive yields

$$V_{ac} > \frac{1}{2\Omega} \left| \frac{gz_o}{(q/m)} - CV_g \right| \left[\Omega^2 + \left(\frac{C_d}{m}\right)^2\right]^{1/2}$$

$$+\left\{ \left[\left| \frac{gz_o}{(q/m)} - CV_g \right| \left(\Omega^2 + \left(\frac{C_d}{m}\right)^2\right) \right] \left[\left| \frac{gz_o}{(q/m)} - CV_g \right| \frac{1}{4\Omega^2} + \frac{z_o^2}{2(q/m)} \right] \right\}^{1/2} \quad (2.42)$$

For expected values of (q/m) and appropriate adjustment of V_g, we may minimize the importance of this criterion. We note however that in practice it is impossible to adjust V_g such that V_g is exactly equal to $gz_o m/Cq$, for which any positive value of V_{ac} will satisfy Eq. (2.42).

Let γ be the smallest fractional error in V_g that is practically possible, such that the balancing voltage is $V_g = (1-\gamma) \frac{gz_o}{C(q/m)}$. Substituting into Eq. (2.42) requires that

$$V_{ac} > \frac{1}{2\Omega} \left[\frac{\gamma g z_0}{(q/m)} \right] \left[\Omega^2 + \left(\frac{C_d}{m}\right)^2\right]^{1/2}$$

$$+ \left\{ \left[\left(\frac{\gamma g z_o}{(q/m)}\right) \left(\Omega^2 + \left(\frac{C_d}{m}\right)^2\right) \right] \left[\left(\frac{\gamma g z_o}{(q/m)}\right) \frac{1}{4\Omega^2} + \frac{z_o^2}{2(q/m)} \right] \right\}^{1/2} \quad (2.43)$$

From Eq. (2.43), we note that the more sensitive the adjustment of V_g, the lower the required value of V_{ac}.

2.3.3 Required Behaviour of Particle after Removal of an Electron

For practical reasons, we require that, after removal of an electron, (i) the particle remain within the chamber, and (ii) the movement of the particle from the chamber center be clearly visible in a microscope.

The first requirement specifies that the sum of the

displacement of the center of motion and the amplitude of oscillation be less than δz_0, where δ is a constant less than 1. Using Eq. (2.37), we solve the quadratic for V_{ac} to obtain

$$V_{ac} > \frac{z_0 gm}{2\delta\Omega\epsilon n(n+1)} \left[\Omega^2 + \left(\frac{C_d}{m}\right)^2\right]^{1/2}$$

$$+ \frac{z_0 m}{\epsilon n} \left(\frac{g}{\delta(n+1)}\right)^{1/2} \left[\left(\Omega^2+\left(\frac{C_d}{m}\right)^2\right)\left(\frac{g}{4\delta\Omega^2(n+1)} + \frac{z_0}{2}\right)\right]^{1/2} \qquad (2.44)$$

The second requirement specifies that the sum of the displacement of center of motion and the amplitude of oscillation be greater than about $\zeta = 10^{-4}$m. Thus

$$V_{ac} < \frac{z_0^2 gm}{2\zeta\Omega\epsilon n(n+1)} \left[\Omega^2+\left(\frac{C_d}{m}\right)^2\right]^{1/2}$$

$$+ \frac{z_0^2 m}{\zeta^{1/2}\epsilon n} \left(\frac{g}{n+1}\right)^{1/2} \left[\left(\Omega^2+\left(\frac{C_d}{m}\right)^2\right)\left(\frac{g}{4\zeta\Omega^2(n+1)} + \frac{1}{2}\right)\right]^{1/2} \qquad (2.45)$$

For $\delta < 1$, the particle will remain in the chamber after electron stepping. Because of the large drag on small particles, such particles move slowly to their new positions of equilibrium; the drift velocity is inversely proportional to the drag. Thus it is possible to adjust V_g immediately after removal of an electron and before the particle has drifted out of the chamber. Therefore it may be possible for δ to be greater than one and the chamber to be still useful. Calculation of values of $\left(\frac{C_d}{m\Omega}\right)$ for particles less than about 5 μm in diameter shows that $\left(\frac{C_d}{m\Omega}\right) >> 1$ for Ω less than approximately 10^4 to 10^5 Hz. Eqs. (2.43), (2.44) and (2.45) show that with $\left(\frac{C_d}{m\Omega}\right) >> 1$, the design criteria are essentially independent of Ω.

2.4 Calculation of Particle Mass

As shown by Eq. (2.35), a particle with an initial charge-

to-mass ratio (q_i/m) will be balanced at the null point for

$$V_{g_i} = \frac{gz_0}{C(q_i/m)} \tag{2.46}$$

where C is a geometric constant. If a single elementary charge is removed or added to the particle such that it has a final charge to mass ratio (q_f/m), the final balancing voltage is

$$V_{g_f} = \frac{gz_0}{C(q_f/m)} \tag{2.47}$$

Thus
$$q_i - q_f = \pm \varepsilon = g \frac{z_0 m}{C} \left(\frac{1}{V_{g_i}} - \frac{1}{V_{g_f}}\right) \tag{2.48}$$

where ε is the elementary unit of charge, and therefore

$$m = \frac{C\varepsilon}{gz_0} \left| \frac{V_{g_i} V_{g_f}}{V_{g_f} - V_{g_i}} \right| \tag{2.49}$$

Thus knowledge of the balancing voltage V_g before and after electron stepping allows direct calculation of the particle mass based only on physical constants without any calibration requirements.

2.5 Geometric Constant for the Endcap DC Field

When a particle is balanced at the null point, we have

$$V_g = \frac{gz_0}{C(q/m)} \tag{2.50}$$

The constant C is a function of the chamber geometry and is identically 0.5 for infinite flat plates. However, the quadrapole employs hyperboloidal endcaps.

Attempts to obtain an analytical solution to the field due to the hyperboloidal endcaps were not successful. As far as the author is aware, no such solution is reported in the

literature. The solution in spherical co-ordinates to the governing Laplace's Equation for an axisymmetric field is given by (42)

$$V(r_s,\theta) = \sum_{n=0}^{\infty} [A_n r_s^n + B_n \frac{1}{r_s^{n+1}}] P_n(\cos\theta) \qquad (2.51)$$

where r_s is the radius in spherical co-ordinates, the P_n are Legendre Polynomials and the A_n and B_n are determined by boundary conditions. Since the field is to remain finite between the endcaps at $r_s = 0$, we require the B_n's to be identically zero, leaving only the A_n's to be determined from the shape of the endcaps. A finite element method was employed to solve for the field at the chamber center, using a computer code developed by Brown (43). This yielded

$$C = \frac{z_0 E_g}{V_g} \approx 0.4 \qquad (2.52)$$

Since at the null point (neglecting particle buoyancy)

$$mg = qE_g \qquad (2.53)$$

we have

$$V_g = \frac{gz_0}{(0.4)(q/m)} \qquad (2.54)$$

3. EXPERIMENTAL

3.1 Aerosol Generation

Aerosol was generated by a De Vilbiss No. 40 Nebuliser, the output characteristics of which have been reported by Mercer et al. (44). A 10% by volume suspension of Dow Diagnostics Uniform Latex Particles in water was diluted by a factor of about 125 and placed in the nebuliser reservoir. This dilution is well above the factor of about 50 calculated by Raabe (45) to ensure that almost all the water droplets generated by the nebuliser contain at most one latex particle. Deionized water was used throughout. The air was supplied from Matheson Dry Air cylinders and was fed through a Matheson 452 Oil and Water Filter and a 6164 High Purity Filter before reaching the nebuliser. Air flow rates to aerosolize the particle suspension were from 0.05 ℓs^{-1} to 0.08 ℓs^{-1}, controlled through a rotameter and stopcock.

The stream of droplets from the nebuliser was passed through a drying tube consisting of a 0.3 m long and 35 mm diameter Pyrex tube. Along its axis the tube contained a 15 mm diameter wire mesh cylinder through which the aerosol stream flowed. The annular space between the glass tube and wire cylinder was filled with 8 mesh indicating Drierite. The color change of the dessicant as seen through the outer glass tube indicated when the dessicant charge should be replaced. After the drying tube, the aerosol stream was fed directly to the chamber. As far as possible, glass tubing was used for connections from the nebuliser to the chamber.

The nebuliser produced a wide range of charge-to-mass ratios. Using 2.35 μm diameter latex spheres, charge-to-mass ratios of about 0.10 to 0.001 coulombs kg^{-1} were produced. The charge-to-mass ratio on the particles could be increased and limited to higher values by inducing additional charge on the particles. An insulated 22 ga. solid core wire was inserted in the nebuliser and positioned about 1 mm from the spray jet. A second uninsulated wire was inserted into the nebuliser reservoir. A constant voltage was then applied to the two wires. If the spray jet wire was made positive with respect to the reservoir wire, negatively charged particles resulted and vice versa. This system produced a much narrower range of charge-to-mass ratios. Using 2.35 μm particles, charge-to-mass ratios of about 0.15 to 0.02 coulombs kg^{-1} were produced. Two sizes of Dow Diagnostics Uniform Latex Particles were used, as shown in Table 3.1 (46).

3.2 Electrical System

The circuitry to produce the ac voltage (with dc bias) on the ring electrode and the dc voltage across the endcaps is given in Figure 3.1. The capacitor-resistor networks suppress induced ac voltages resulting from the ac voltage on the ring electrode. The regulated dc power supply to produce V_g across the endcaps consisted of a Pacific Instruments 7104 P.C. Card with an off-board 10-turn potentiometer connected in series with a Power Designs 2015 R power supply equipped with a coarse and fine adjustment. This system was capable of producing 0 to 2020 V across the endcaps with a resolution of 0.005 V. The power transformers were Essex Stancor P-8151

TABLE 3.1

Calibration Particles Used in this Work

Mean Diameter (μm)	Standard Deviation (μm)	Material	Density (kg m^{-3})	Lot No.
0.497	0.0059	Polystyrene	1050	1A06
2.350	0.0197	Polyvinyltoluene	1027	8C25

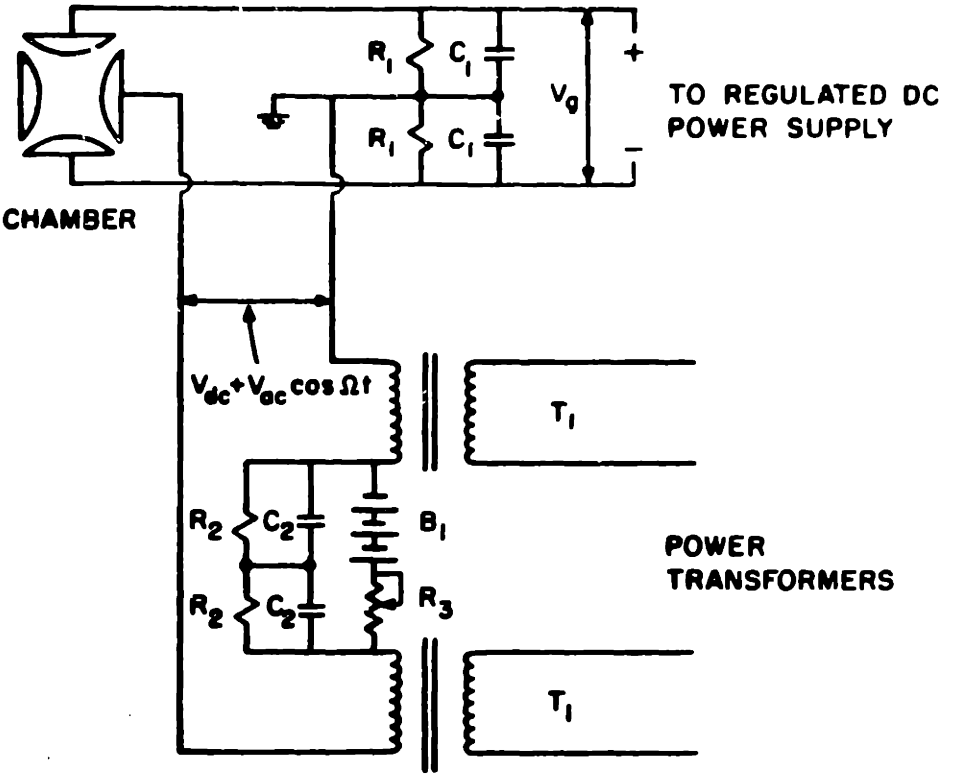

R_1 = 196 kΩ C_1 = 0.47 MFD 400 WVDC

R_2 = 81 kΩ C_2 = 0.0068 MFD 200 WVDC

T_1 = 2400 VAC POWER TRANSFORMER 110 V 60 Hz

B_1 = 3 X 45 V BATTERIES IN SERIES

R_3 = 0.5 MΩ

FIG. 3.1 CIRCUITRY FOR QUADRAPOLE

2400 VAC CRT transformers and the dc bias on the ring electrode was provided by 3 Eveready 762-S 45 V batteries connected in series and provided with a 0.5 MΩ variable resistor. The power transformers were controlled by a Powerstat 3PN116B Variable Transformer which gave a near linear output of 0 to 140 VAC. The ring electrode system provided a dc bias of 0 to 135 V with a resolution of 0.5 V and an rms ac voltage of 0 to 4800 V at 60 Hz with a resolution of about 50 V. For safety, Belden 25 kV CRT wire was used. Measurements of V_g were made with a Keithley 192 Digital Multimeter capable of reading up to 6 1/2 digits. The meter was protected by a 30 mA fuse on the negative lead.

3.3 Optical Equipment

Illumination was provided by a Spectra Physics Stabilite™ Model 120-S 15 mW He-Ne Laser having a beam width of 0.8 mm. The laser was fitted with an Oriel Beam Aligner and was mounted on an Oriel 5 inch Rotating Stage attached to a vertical optical bench. This mounting allowed the laser beam to be directed into the chamber along the asymptote between the electrodes as described in Section 3.5. The particles were observed through a flat glass window using an Ealing microscope equipped with a widefield eyepiece and capable of providing up to 30 x magnification. The microscope was attached to an Oriel tilting head mounted on a traversing stage positioned on an optical rail. UV light was provided by an Oriel 6035 low pressure mercury calibration lamp equipped with a pinhole shield. The chamber, laser mounting and microscope mounting were all fixed to an

optical base plate, which prevented movement of the laser, chamber and microscope relative to each other.

3.4 The Quadrapole

The quadrapole used in the present work had characteristic dimension z_o = 4 mm. The chamber consisted of a central ring electrode of aluminum and two Teflon rings on either side. The two aluminum endcap electrodes were mounted in the Teflon rings. Holes were drilled into the Teflon rings between the ring and endcap electrodes to allow access to the chamber. The aerosol stream was fed through one hole and the hole directly opposite the aerosol inlet was used as the gas exhaust. The UV light source was positioned at another hole so as to irradiate the chamber through that hole. The laser beam was directed through the chamber center through an additional pair of holes and the chamber center was viewed through another hole. The laser exit and entry holes and the viewing hole were sealed by flat glass windows, while the pinhole shield of the UV light source sealed the hole at which the UV light source was positioned. All the abovementioned holes were drilled into the Teflon spacing rings and were positioned along the asymptotes so as to avoid drilling holes in the electrodes themselves. Holes in the electrodes would lead to distortions in the electric fields in the chamber. The chamber geometry is such that a particle can "see" only the electrodes and the Teflon at the gap between the electrodes. Glass windows were used since Plexiglass tends to maintain a residual surface charge, which could distort the field within the chamber. The entire chamber was positioned within a grounded closed metal cylinder, which

prevented external electric fields from disturbing the chamber fields and also prevented accidental contact with the high voltage electrodes.

3.5 Experimental Procedure

A diluted suspension of latex particles was placed in the nebuliser reservoir and the constant voltage across the leads to the nebuliser adjusted as desired. The laser alignment was checked, as were all electrical contacts. The ring voltage was adjusted as desired, usually in the range of 2 to 2.5 kV with no additional dc bias. The voltage across the endcaps was set to its minimum value, typically about 0.3 V. The air flow to the nebuliser was turned on at the rotameter and adjusted as desired. After a short period, the air flow was shut off as quickly as possible. This often left some particles in the chamber, and these particles were then held by the chamber fields. A particle which responded suitably to application of V_g to the endcaps was then balanced roughly at the chamber center. The ring ac voltage was then lowered for a couple of seconds. This usually allowed the unbalanced particles to fall out of the chamber while the nearly balanced particle remained near the chamber center. The ac voltage was then increased again. If only the particle of interest remained, it was more carefully balanced by adjusting V_g and then lowering the ac voltage for a couple of seconds. If the particle drifted from the chamber center, it was clearly unbalanced. The ac voltage was then increased again and V_g further adjusted, after which the procedure was repeated, until, on lowering and raising the ac voltage

the particle did not move. This signified that the particle was now balanced and so V_g was recorded. The UV light was then turned on for a few seconds and the particle observed closely. The onset of particle drift from the chamber center and subsequent oscillation indicated that the particle had lost at least one electron. This was confirmed by lowering the ac voltage for a short time, in response to which the particle would drift downward, as discussed in Chapter 2. The particle was then rebalanced at the chamber center by the technique already described and V_g again recorded. From these two values of V_g the particle mass was directly calculated as discussed in Chapter 2. This electron stepping technique was repeated several times on each particle to confirm the removal of just a single electron and to provide additional mass measurements for statistical purposes.

Photographs of the experimental configuration and the chamber components are presented in Figs. 3.2 to 3.4.

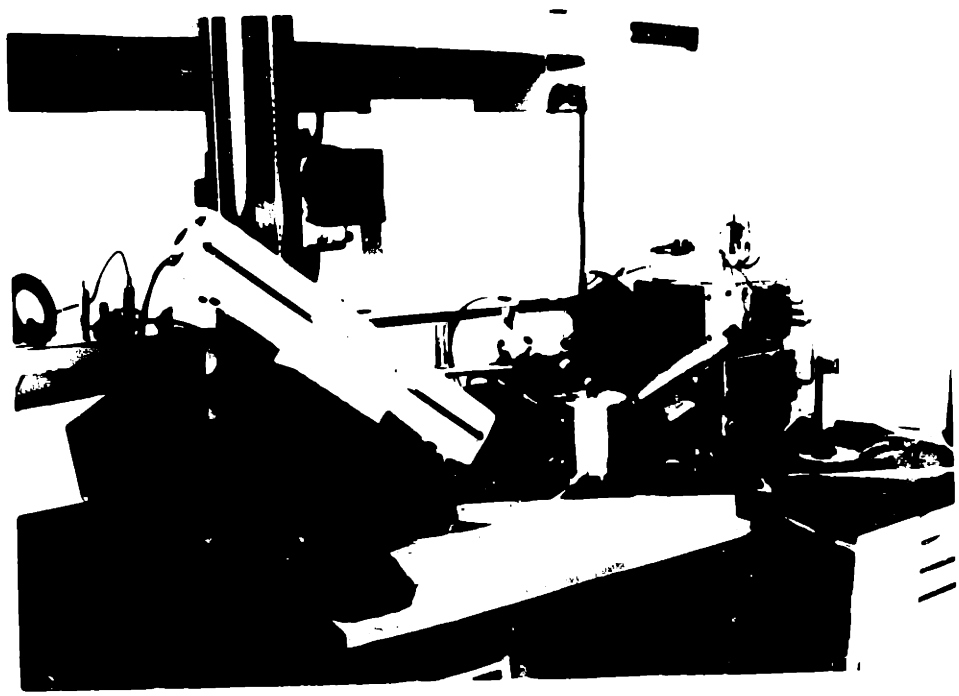

Fig. 3.2 Layout of equipment, showing laser and mounting, power supplies, microscope, UV light, aerosol delivery apparatus and quadrapole.

INTENTIONAL DUPLICATE EXPOSURE

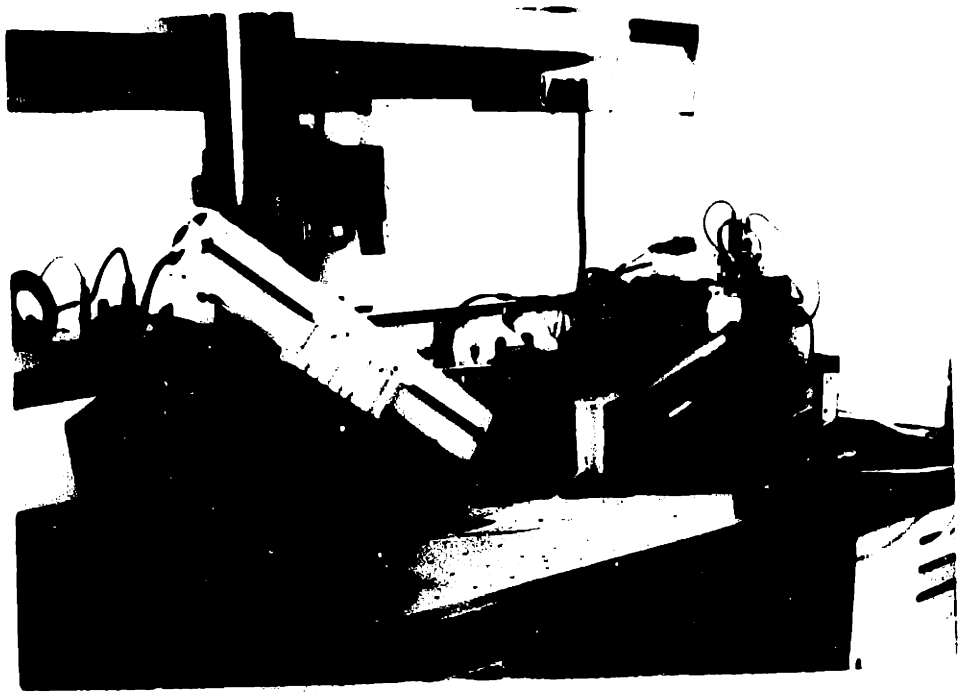

Fig. 3.2 Layout of equipment, showing laser and mounting, power supplies, microscope, UV light, aerosol delivery apparatus and quadrapole.

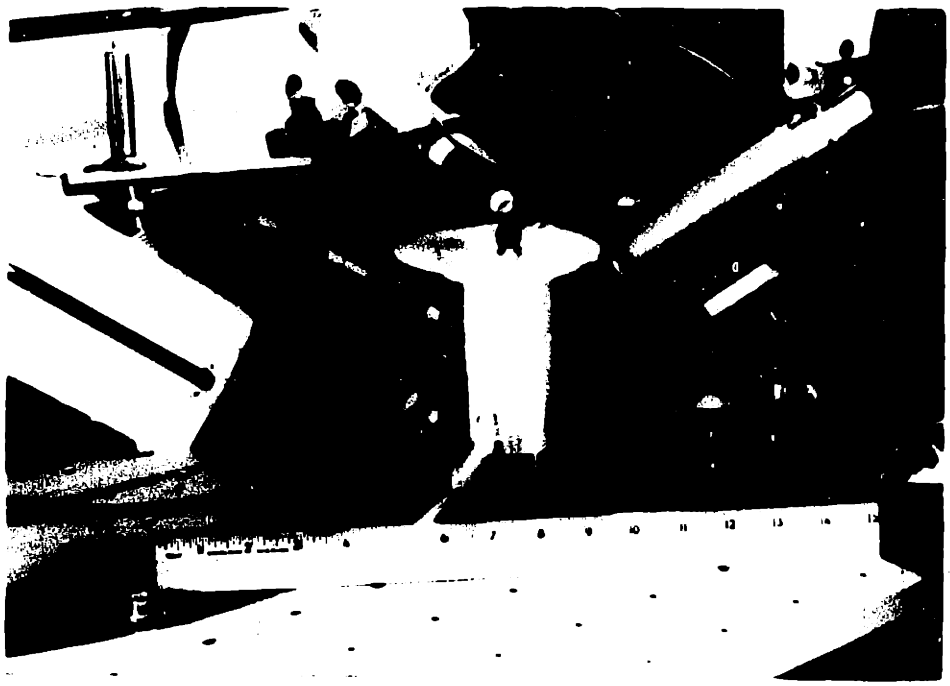

Fig. 3.3 Close up of quadrapole, showing laser aligner, UV light, microscope and drying tube for the aerosol stream.

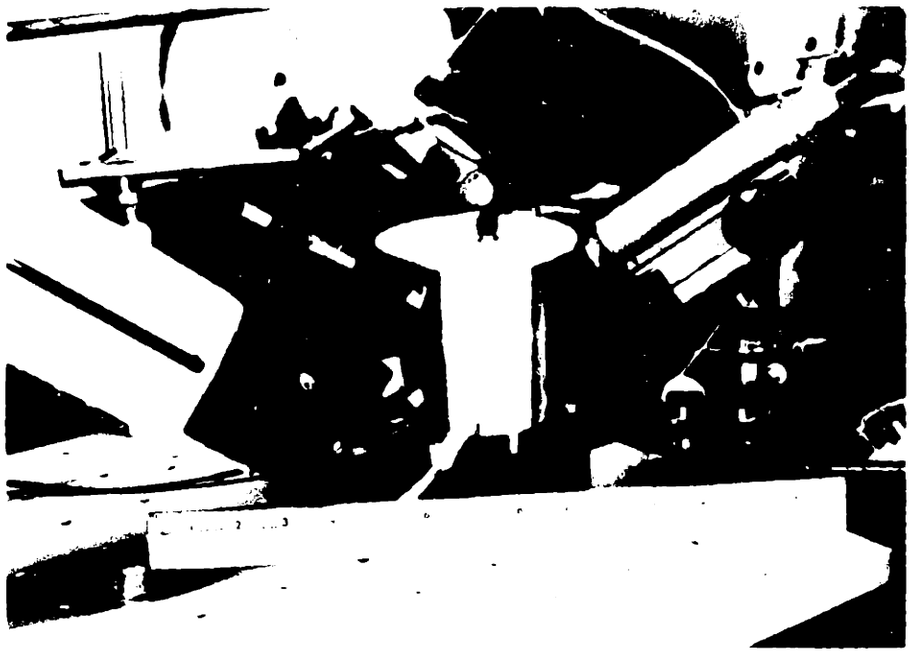

Fig. 3.3 Close up of quadrapole, showing laser aligner, UV light, microscope and drying tube for the aerosol stream.

INTENTIONAL DUPLICATE EXPOSURE

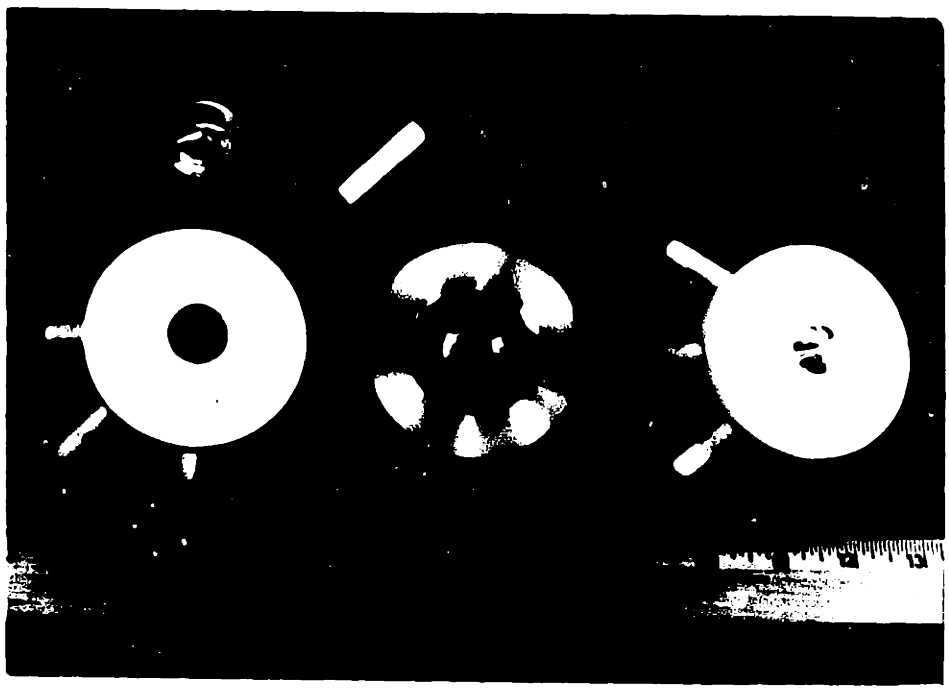

Fig. 3.4 Disassembled quadrapole, showing Teflon spacer rings, endcap electrodes, glass window, Teflon port and central ring electrode.

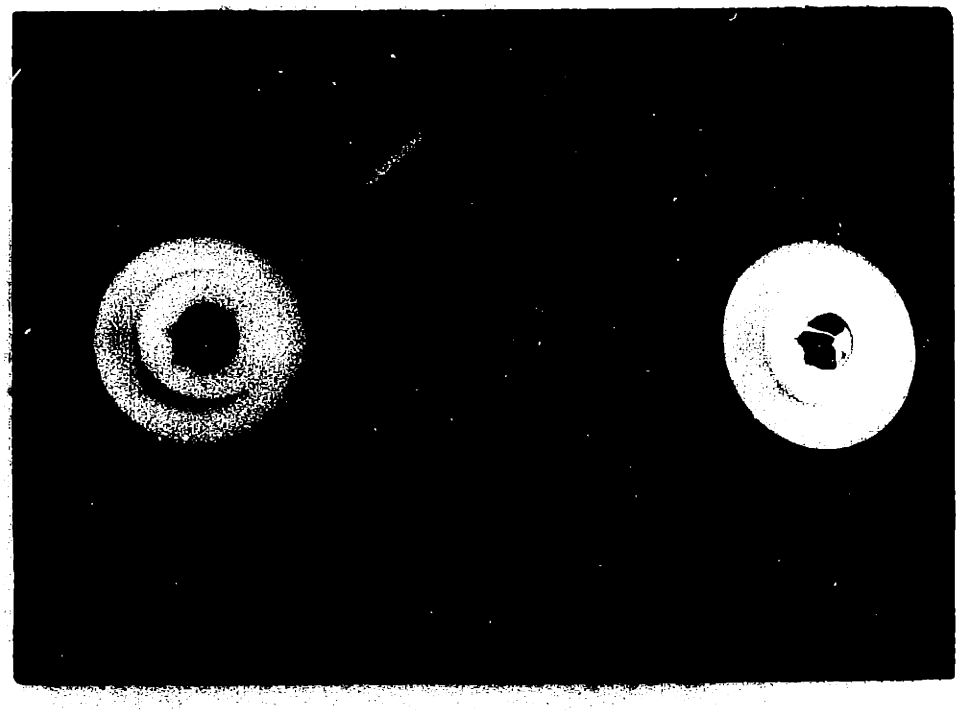

Fig. 3.4 Disassembled quadrapole, showing Teflon spacer rings, endcap electrodes, glass window, Teflon port and central ring electrode.

4. RESULTS

Particles of known mass were weighed in the quadrapole to confirm the technique of electron stepping in a quadrapole. The mass of the 2.35 μm diameter particles was determined in the quadrapole described above while the mass of the 0.497 μm diameter particles was determined during preliminary testing of a quadrapole with z_o = 4.49 mm loaned by Prof. Steven Arnold of the Polytechnic Institute of New York. The data and analysis thereof are presented in Table 4.1.

Analysis of the mean mass measurements for the 2.35 μm diameter particles yields a measured particle diameter of 2.339 $\pm$ 0.014 μm.

TABLE 4.1

Manufacturer's Stated Particle Mass (kg)	Sucessive Values of V_g (volts)	Change in Voltage (Volts)	Calculated mass (kg)	Calculated Number of Elementary Charges
$(6.979\pm0.177)\times10^{-15}$	60.13	-	-	71.2
(2.35 μm)	62.70	2.57	7.187×10^{-15}	68.3
	63.68	0.98	6.653×10^{-15}	67.2
	65.71	2.03	6.732×10^{-15}	65.1
	66.71	1.00	7.158×10^{-15}	64.2
	68.89	2.18	6.885×10^{-15}	62.1
	69.95	1.06	7.424×10^{-15}	61.2
	71.14	1.19	6.829×10^{-15}	60.2
		Mean:	$(6.981\pm0.280)\times10^{-15}$	
	94.86	-	-	45.3
	97.00	2.14	7.021×10^{-15}	44.3
	99.19	2.19	7.174×10^{-15}	43.4
	104.06	4.87	6.922×10^{-15}	41.3
	106.64	2.58	7.024×10^{-15}	40.2
	109.38	2.75	6.927×10^{-15}	39.3
		Mean:	$(7.014\pm0.102)\times10^{-15}$	
	66.34	-	-	63.2
	67.39	1.05	6.953×10^{-15}	62.2
	69.67	2.28	6.725×10^{-15}	60.2
	70.84	1.17	6.889×10^{-15}	59.2
	72.04	1.20	6.945×10^{-15}	58.2
	74.63	2.59	6.780×10^{-15}	56.1
	76.00	1.37	6.761×10^{-15}	55.2
		Mean:	$(6.842\pm0.099)\times10^{-15}$	
$(6.749\pm0.243)\times10^{-17}$	10.11	-	-	4.2
(0.497 μm)	12.33	2.22	8.171×10^{-17}	3.4
	16.46	4.13	7.150×10^{-17}	2.6
		Mean:	$(7.661\pm0.722)\times10^{-17}$	
	4.73	-	-	8.9
	5.16	0.43	8.259×10^{-17}	8.1
	5.72	0.56	7.669×10^{-17}	7.3
	6.50	0.78	6.935×10^{-17}	6.4
		Mean:	$(7.621\pm0.663)\times10^{-17}$	

5. DISCUSSION AND CONCLUSIONS

The development of electron stepping in a quadrapole represents a significant improvement in our ability to measure temporal variations in particle mass. The specific advantages over previous techniques (14,30) are that 1) knowledge of material density is not necessary, 2) the particle charge need not remain constant between mass measurements, 3) no independent measurement of initial particle mass is required and 4) no adjustable parameters are required. Arnold's technique (15) of electron stepping provides direct measurement of particle mass, but requires a feedback system. While a feedback system is not necessary for the quadrapole, inclusion of such a system would allow automatic unattended data acquisition for particle mass measurement. The system may be automated by a computer, which could be used to balance a particle through a feedback system and irradiate the particle with UV light at some specified time interval. Automatic rebalancing and recording of particle mass as a function of time would facilitate use of the instrument for extended measurements over a period of several hours.

From Table 4.1 we see that for 2.35 μm diameter particles, excellent reproducibility is obtained with sucessive measurements on the same particle. In addition, excellent agreement is obtained for all particles of the same size and the mean mass measurement for each particle lies well within the standard deviation given by the manufacturer. While the measurements of the 0.497 μm diameter particles are reproducible, the mean mass measurements lie outside the standard deviation given by

the manufacturer. The error in the calculated mass is about 12%. These measurements were obtained during preliminary testing in Arnold's chamber, which has four symmetrically placed ∿ 3 mm diameter holes drilled through the ring electrode . It was noted that particles often tended to drift towards one of the holes, raising the possibility of distortion of the focussing field due to these holes. Considering the difficulty in judging the balancing voltage with these 0.497 μm particles, as discussed later, and also the possible distortion of the focussing field, it was encouraging to obtain agreement within about 12% of the manufacturer's stated particle size. Tests on 0.497 μm particles will be performed in the new chamber, which has no holes in any of the elctrodes. It should be noted that non-integral values are calculated for the number of charges on a particle. Clearly, non-integral values are not possible and thus the calculated values presented provide some estimate of the errors in the data. There are several possible sources of error. First, the geometric constant C as given in Eq. (2.10) was calculated to be 0.4 only to within about one percent. By using more computer time for a more refined computational mesh, one may improve the accuracy of this number. Second, the determination of the balancing voltage V_g is subjective in that the experimenter must visually judge when a particle is balanced. The instability of the power supplies limits the number of reliable decimal places and the truncated values of V_g used for computation add to the errors in the balancing voltage. Clearly a computer controlled feedback

system and better power supplies would reduce this error.

It should be noted that considerable difficulty was encountered in feeding charged 2.35 μm diameter particles into the chamber. Several hours of manipulation of the aerosol delivery system was often necessary before a particle was fed into the chamber and trapped by the focussing field. However, feeding 0.497 μm diameter particles was considerably easier. Possibly the large 2.35 μm particles are lost by impaction on a bend in the glass tube feeding the aerosol stream into the chamber. Once a 2.35 μm diameter particle had been trapped in the chamber, measurement of its mass was relatively simple. Normally one mass determination could be made in one minute. In contrast, considerable difficulty was encountered in weighing 0.497 μm diameter particles. Visual observation was more difficult and because of the large drag on these particles, they moved very slowly, making it difficult to determine if the particle was balanced. These difficulties may partially account for the mean mass measurements for these particles lying outside the standard deviations given by the manufacturer. Additional mass measurements on the same particle could easily have been taken in the chamber without holes in the electrodes. However, data for the 0.497 μm diameter particles were taken in the chamber with holes in the electrodes and additional measurements were not taken because the particle was lost. Thus the agreement to within only 12% obtained with the 0.497 μm diameter particles cannot be taken as a measure of the capabilities of the quadrapole.

Now that the feasibility of electron stepping in a quadrapole has been demonstrated, many areas of application are envisioned. For example, there is much interest in the mechanisms of gas-to-particle conversion. Specifically, the conversion of gaseous sulfur dioxide to a sulfate aerosol has received considerable attention. Although much work has been reported (1-13, 16-23) on the inhibitive and catalytic effects of trace gases such as NH_3, O_3, NO_2, CO, N_2O and the crucial part played by aerosols, which provide sites for adsorption and catalytic reaction of reactant gases, a complete mechanistic explanation for these processes is still unavailable. Application of the experimental techniques developed in this work may help in elucidating the complex mechanisms of gas-to-particle conversion.

It should be noted that this work is the first reported direct measurement of aerosol particle mass in a quadrapole using electron stepping. Because no *a priori* assumptions are required about the particle to be weighed, this technique has wide application in aerosol particle studies which require suspension of a single particle in a controlled gaseous environment. The techniques employed i this work may now serve as a basis for future studies on the growth, evaporation and heterogeneous reactions of aerosol particles.

APPENDIX A

The Field E_g due to the Potential Difference V_g Across the Endcap Electrodes

The solution to Laplace's Equation in spherical co-ordinates for a radially symmetric field that is finite everywhere is given by

$$V(r_s,\theta) = \sum_{n=0}^{\infty} [A_n r_s^n P_n(\cos\theta)] \qquad (A.1)$$

where the P_n are Legendre Polynomials and the A_n are determined by boundary conditions.

The potential due to V_g across the endcaps contains only the odd terms in the expansion Eq.(A.1). Therefore

$$V_g(r_s,\theta) = A_1 r_s \cos\theta + \frac{A_3}{3} r_s^3 (5\cos^3\theta - 3\cos\theta) + \ldots \qquad (A.2)$$

Rewriting Eq. (A.2) in terms of cylindrical co-ordinates r and z as defined by Fig. 2.1 and differentiating partially gives E_g in the r and z directions:

$$E_{g_z} = \bar{A}_1 + \bar{A}_3(r^2 - 2z^2) + \ldots \text{ higher order terms} \qquad (A.3)$$

$$E_{g_r} = 2\bar{A}_3 rz + \ldots \text{ higher order terms} \qquad (A.4)$$

where the $\bar{A}_n$ are linear functions of the A_n. Therefore the $\bar{A}_n$ are determined by the boundary conditions, in this case the value of V_g.

We note that for small values of r and z we may neglect the field in the r direction and approximate the field E_g by

$$E_{g_z} = \bar{A}_1 \tag{A.4}$$

Eq. (A.4) is exact only for $r = z = 0$. For $r \neq 0$, $z \neq 0$ Eq. (A.4) is only an approximation. Along $r = 0$, $E_{g_r} = 0$ and the field has a component in the z direction only. Noting this, and that $\bar{A}_1$ is determined by V_g, we write

$$E_g = \frac{CV_g}{z_0} \tag{A.5}$$

and take it to have a component in the z direction only. C is a geometric constant and z_0 is the characteristic dimension of the chamber.

REFERENCES

1. Hegg, D.A., and Hobbs, P.V.,"Oxidation of Sulfur Dioxide in Aqueous Systems with Particular Reference to the Atmosphere" Atmospheric Environment 12, 241 (1978).

2. Cofer, W.R., Schryer, D.R., and Rogowski, R.S., "The Enhanced Oxidation of SO_2 by NO_2 on Carbon Particulates" Atmospheric Environment 14, 571 (1980).

3. Chang, S.G., and Novakov T., "Soot Catalysed Oxidation of Sulfur Dioxide from Man's Impact on the Troposphere" NASA Publ. 1022 (1978).

4. Judeikis, H.S., and Siegel, S., "Particle Catalyzed Oxidation of Atmospheric Pollutants" Atmospheric Environment 7, 619 (1973).

5. Johnstone, H.F., and Coughanowr, D., "Adsorption of Sulfur Dioxide from Air" Ind. Eng. Chem. 50, 1169 (1958).

6. Britton, L.G., and Clarke, A.G., "Heterogeneous Reactions of Sulfur Dioxide and SO_2/NO_2 Mixtures with a Carbon Scot Aerosol" Atmospheric Environment 14, 829 (1980).

7. Liberti, A., Brocco, D., and Possanzini, M., "Adsorption and Oxidation of Suflur Dioxide on Particles", Atmospheric Environment 12, 255 (1978).

8. Judeikis, H.S.,Stewart, T.B., and Wren, A.G., "Laboratory Studies of Heterogeneous Reactions of SO_2" Atmospheric Environment 12, 1633 (1978).

9. Corn, M., and Cheng, R.T., "Interaction of Sulfur Dioxide with Insolube Suspended Particulate Matter" J. Air Pollut. Control Ass. 22, 870 (1972).

10. Chun, K.C., and Quon, J.E., "Capacity of Ferric Oxide Particles to Oxidize Sulfur Dioxide in Air" Envir. Sci. Technol. 7, 532 (1973).

11. Dyson, W.L., and Quon, J.E., "Reactivity of Zinc Oxide Fume with Sulfur Dioxide in Air" Envir. Sci. Technol. 10, 476 (1976).

12. Smith, B.M., Wagman, J., and Fish, B., "Interaction of Airbourne Particles with Gases" Envir. Sci. Technol. 6, 558 (1969).

13. Haury, G., Jordan, S.,and Hofman, C.,"Experimental Investigation of the Aerosol-Catalyzed Oxidation of SO_2 Under Atmospheric Conditions" Atmospheric Environment 12, 281 (1978).

14. Davis, J.E., and Ray, A.K., "Single Aerosol Particle Size and Mass Measurements Using an Electrodynamic Balance" Journal of Colloid and Interface Science 75, 566 (1980).

15. Arnold, S., "Determination of Particle Mass and Charge by One Electron Differentials" J. Aerosol Sci. 10, 49 (1979).

16. Matteson, M.J., Stober, W., and Luther, H., "Kinetics of the Oxidation of Sulfur Dioxide by Aerosols of Manganese Sulfate" I&EC Fundam. 8, 677 (1969).

17. Overton, J.H., Aneja, V.P., and Durham, J.L., "Production of Sulfate in Rain and Raindrops in Polluted Atmospheres" Atmospheric Environment 13, 355 (1979).

18. Fox, D.G., "Precipitation Quality and its Effects on Stream Water Quality and the Forest in General". Symp.: Non-Point Sources Pollut. For. Land., Proc. Meet. 103 (1977)

19. Hill, F.B., and Adamowicz, R.F., "A Model for Rain Composition and the Washout of Sulfur Dioxide" Atmospheric Environment 11, 917 (1977).

20. Hidy, G.M., Katz, J.L., and Mirabel, P., "Sulfate Aerosol Formation and Growth in the Stratosphere" Atmospheric Environment 12, 887 (1978).

21. Scott, W.D., and Hobbs, P.V., "The Formation of Sulfate in Water Droplets" Journal of the Atmospheric Sciences 24, 54 (1967).

22. Mackay, H.A.C.,"The Atmospheric Oxidation of Suflur Dioxide in Water Droplets in the Presence of Ammonia" Atmospheric Environment 5, 7 (1971).

23. Cofer, W.R., Schryer, D.R., and Rogowski, R.S., "The Oxidation of SO_2 on Carbon Particles in the Presence of O_3, NO_2 and N_2O" Atmospheric Environment 15, 1281 (1981).

25. Paul, W., and Raether, M., Z. Phys. 140, 262 (1953).

26. Fischer, E., Z. Phys. 156, 1 (1959).

27. Weurker, R.F., Shelton, H., and Langmuir, R.V., "Electrodynamic Containment of Charged Particles" Journal of Applied Physics 30, 342 (1959).

28. Blau, H.H., McCleese, D.J., and Watson, D., "Scattering by Individual Transparent Spheres" Applied Optics 9, 2522 (1970).

29. Frickel, R.H., Shaffer, R.E., and Stamatoff, J.B., "Chambers for the Electrodynamic Containment of Charged Aerosol Particles" Tech. Report ARCSL-TR77041. U.S. Army Armament Research and Development Command, Aberdeen, Maryland (1978).

30. Ray, A.K., Ph.D. Thesis, Dept. of Chemical Engineering, Clarkson College of Technology, Potsdam, N.Y. (1980).

31. Arnold, S., Private Communication.

32. McLachlan, N.W., "Theory and Applications of Mathieu Functions" Oxford University Press, New York (1947).

33. Zaroodny, S.J., "An Elementary Review of the Mathieu-Hill Equation of Real Variable Based on Numerical Solutions" Ballistic Research Laboraties Memo. Report 876, Aberdeen, Maryland (1955).

34. Marion, J.B., "Classical Electromagnetic Radiation" Academic Press, New York (1965).

35. Friedlander, S.K., "Smoke, Dust and Haze", John Wiley, Chapter 9 (1977).

36. Gelbard, F. and Seinfeld, J.H. "Exact Solution of the General Dynamic Equation for Aerosol Growth by Condensation" J. Colloid and Interface Science 68, 173 (1979).

37. Peterson, T.W. and Seinfeld, J.H. "Mathematical Model for Transport, Interconversion, and Removal of Gaseous and Particulate Air Pollutants - Application to the Urban Plume", Atmospheric Environment 11, 1171 (1977).

38. Peterson, T.W., and Seinfeld, J.H., "Calculation of Sulfate and Nitrate Levels in a Growing, Reacting Aerosol", AIChE Journal 25, 831 (1979).

40. Wyatt, P.J. and Phillips, D.T., "A New Instrument for the Study of Individual Aerosol Particles", J. Colloid Interface Science 39, 125 (1972).

41. Wyatt, P.J., "Some Chemical, Physical, and Optical Properties of Fly Ash Particles", Applied Optics 19, 975 (1980).

42. Lorrain, P., and Corson, D.R., "Electromagnetic Fields and Waves" page 163 (2nd Ed.) W.H. Freeman, San Francisco (1970).

43. Brown, R.A., "Finite Element Methods for the Calculation of a Capillary Surface" J. Computational Physics 33, 217 (1979).

44. Mercer, T.F., Goddard, R.F., and Flores, R.L., "Output Characteristics of Several Commercial Nebulisers" Ann. Allergy 23, 314 (1965).

45. Raabe, O.G., "The Dilution of Monodisperse Suspensions for Aerosolization" American Industrial Hygiene Association Journal 29, 439 (1968).

46. Dow Diagnostics Information Sheets on Uniform Latex Particles, Dow Chemical Company, Indianapolis.